General Method for the Transformation of Chord-Length Data to a Local Bubble-Size Distribution

Weidong Liu, Nigel N. Clark, and Ali Ihsan Karamavruc
Dept. of Mechanical and Aerospace Engineering, West Virginia University, Morgantown, WV 26506

Bubble-size distributions influence the behavior of multiphase systems, but are not readily measured directly using probes. The chord lengths may be transformed into bubble sizes by modeling the bubble shapes as ellipsoids. Previous research on the transformation of chord-length data into bubble-size distributions using a numerical backward transformation revealed an instability problem. This problem was overcome by transforming the chord-length data to a local bubble-size distribution directly by using a Parzen window function and summing to yield the whole distribution. The best estimate of the local bubble-size density distribution depends on the Parzen window width that was chosen by proposing a measure of performance. An empirical relationship was also offered to determine the best Parzen window width. Chord lengths were generated using the example of a Rayleigh bubble-size distribution and Monte-Carlo simulation. The window approach transformed the chord lengths back into the bubble-size distribution with good agreement.

Introduction

Gas–liquid, gas–solid, and multiphase systems are used widely for combustion, aeration, and reaction. A prerequisite for a better understanding of those processes is the knowledge of bubble sizes and their distribution in the system, since these factors govern the extent of mixing, circulation, heat and mass transfer, and interfacial area. However, so far there has not been an effective technique available to measure bubble sizes directly or infer their distribution occurring in freely bubbling, three-dimensional multiphase systems. A locally measuring probe usually measures chord lengths of bubbles. Hence, data interpretation must be performed to obtain the required information. Previous work on converting the distribution of chord lengths to the bubble-size distribution in numerical form (Clark and Turton, 1988) has demonstrated an instability problem, particularly with small data sets. The recent analytical approach proposed by Liu and Clark (1995) for processing chord-length data requires that a suitable probability function be chosen first to fit the chord-length data. However, the model form of this function is usually not known, so that it was desirable to develop a new method for data interpretation that was free of the distribution shape assumption.

In the measurement of bubble size, photographing bubbles in two-dimensional beds can obtain the bubble-size distribution directly (Chiba et al., 1975; Lim and Agarwal, 1990), but the question is as to whether hydrodynamic conditions in two-dimensional beds may be compared successfully with those in three-dimensional beds. The X-ray method (Rowe and Matsuno, 1971; Judd and Dixon, 1978) can be used to infer the bubble sizes in three-dimensional beds. However, the width of the bed that is explored by the method is limited by the available ray intensities, and at higher bubble concentrations individual bubbles can no longer be distinguished clearly. In contrast, local measurements at arbitrary points within three-dimensional beds, without restriction of bubble concentration, are only possible by using locally measuring probes such as capacitive probes (Matsen, 1973; Werther and Molerus, 1973), resistive probes (Burgess et al., 1981), optical probes (Oki et al., 1975, 1977; Ishida et al., 1980), and static pressure probes (Sitnai, 1982; Clark et al., 1991). General reviews of probes have been presented by Cheremisinoff (1986) and Clark (1986).

Locally measuring probes usually measure chord lengths that can be used to characterize bubble sizes. The chord

Correspondence concerning this article should be addressed to Dr. N. N. Clark.

length, y, is the product of the time duration of the corresponding pulse of the probe signal and the rise velocity of bubble at that moment. Deduction of bubble size (given as a horizontal radius, R) distribution from a set of chord-length data is not straightforward. Werther (1974a,b), using ellipsoidal bubble shapes, provided the first analysis of the relationship between chord lengths and local bubble sizes. Clark and Turton (1988) explored the relations between the density distribution of chord lengths and the density distribution of bubble sizes for a range of bubble shapes, and proposed a numerical backward transform for inferring the local bubble-size density distribution from the chord-length data. Turton and Clark (1989) extended these techniques to the case of spherical-cap bubbles encountered in fluid beds with bubble rise velocity depending on bubble size. Clark et al. (1992) also provided an analysis in gas–liquid flows where bubble shape changes as a function of bubble size. Liu and Clark (1995) proposed an analytical approach for inferring a bubble-size distribution from a chord-length distribution in closed form, and also described statistical relations between bubble sizes and chord lengths. Lee et al. (1990) employed the truncated normal or log normal functions to evaluate the bubble length (virtually chord length) measured by optical fiber probes at different axial heights under steady-state operation to obtain a best fit by using a Marquardt optimization technique.

The objective of this article is to propose a new nonparametric method with optimal structure for transforming chord-length data to a local bubble-size distribution directly without requiring information on the nature of chord-length distribution, the model form of which is usually unknown.

Analysis

Consider a swarm of gas bubbles rising through a liquid or dense-phase medium around a probe. When a bubble of a specific size (that is, horizontal radius) R travels vertically through the bed, this bubble will intersect the probe tip if the horizontal distance between the bubble center and the probe tip, r, lies between zero and the radius of the bubble R, as shown in Figure 1.

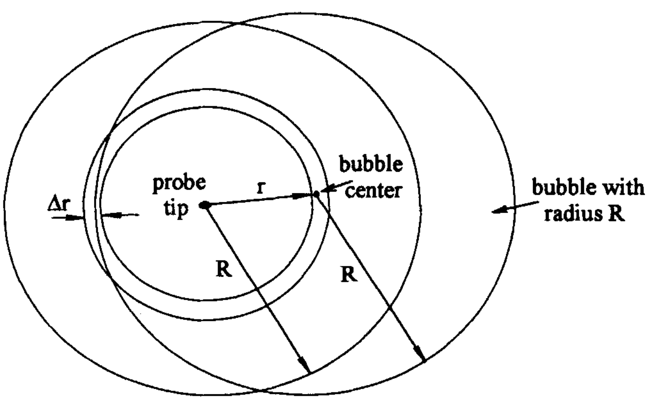

Figure 1. View from top of a bubble, with radius R, rising past a probe.

The bubble will intersect the probe if the distance from the probe to its center $< R$ (according to Clark and Turton, 1988).

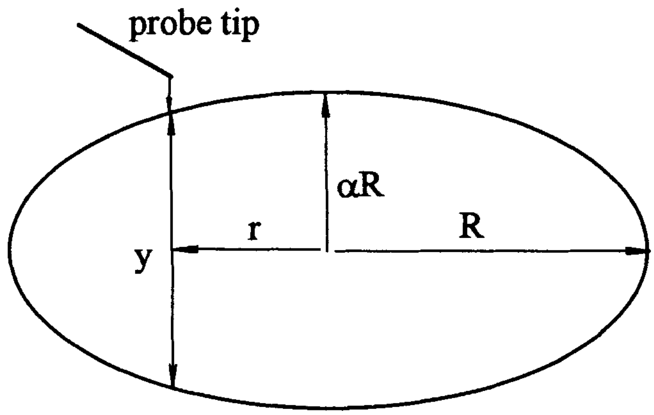

Figure 2. Ellipsoidally shaped bubble model.

The chord length pierced by the probe is usually less than the largest bubble vertical dimension. The chord length varies with the bubble size, the bubble shape, and the distance between the bubble center and the probe. The bubble-shape model employed in this article is the ellipsoidally shaped bubble model that includes the sphere as a special case. This model can be described with parameters R, radius on both of the horizontal (major) axes, and α ($0 < \alpha \leq 1$), a shape factor given by the ratio of the minor (vertical) axis to the two major (horizontal) axes, as shown in Figure 2. For other shape models of bubbles, see Clark and Turton (1988) and Liu and Clark (1995). In the analysis below, α is assumed constant, though the analysis could be pursued with α as a function of bubble size, as was previously examined by Clark et al. (1992). In addition, one must note that bubble shape is dynamic, often oscillatory, and that bubble orientation and rise velocity may not be vertical. These phenomena will serve to introduce error into any idealized analysis, but are not sufficiently well documented for statistical inclusion in a transformation. However, there is a region of bubble sizes where an axisymmetric ellipsoidal model would prove a good representation (Clark et al. 1992).

Chord-length distribution vs. local bubble-size distribution

For vertically rising bubbles of a specific size R, since the chord length is uniquely defined at any radius r from the bubble center, one can derive the conditional probability density function $P_c(y|R)$ for a chord length y pierced by the probe from ellipsoidally shaped bubbles with a size R in a homogeneously bubbling bed or bubble column by using a geometric probability approach. Previously Clark and Turton (1988) showed that

$$P_c(y|R) = \frac{2r}{R^2}\left|\frac{dr}{dy}\right| = \frac{y}{2\alpha^2 R^2}. \qquad (1)$$

The probability of chord lengths occurring for bubbles intersecting the probe with probability density function $P_p(R)$ is given by

$$P_c(y) = \int_0^\infty P_c(y|R)P_p(R)\,dR = \int_{y/2\alpha}^\infty \frac{y}{2\alpha^2 R^2}P_p(R)\,dR. \qquad (2)$$

Equation 2 permits the calculation of the distribution of chord lengths pierced by the probe. For example, if $P_p(R)$ is a gamma distribution, the distribution of the chord lengths is the sum of a set of gamma distributions with weighting coefficients (Liu and Clark, 1995).

In fact, the true bubble-size distribution is rarely known, so that the approach for finding a local bubble-size distribution from available chord-length data is of far greater importance. Consider that $P_c(y)$ and $P_p(R)$ are continuous probability functions, and differentiate both sides of Eq. 2 with respect to y and multiply both sides by y to yield

$$yP_c'(y) = \int_{y/2\alpha}^{\infty} \frac{y}{2\alpha^2 R^2} P_p(R)\, dR - \frac{1}{\alpha} P_p(y/2\alpha). \qquad (3)$$

The first item in the right side of Eq. 3 is identically equal to $P_c(y)$, so that

$$P_p(y/2\alpha) = \alpha[P_c(y) - yP_c'(y)]. \qquad (4)$$

In Eq. 4, $P_p(y/2\alpha)$ is actually associated with the local bubble-size distribution. Let $R = y/2\alpha$ and substitute it into Eq. 4 to yield an analytical backward transform as,

$$P_p(R) = \alpha[P_c(2\alpha R) - 2\alpha R P_c'(2\alpha R)]. \qquad (5)$$

Equation 5 provides the technique for inferring the local bubble-size distribution from the chord-length distribution (Liu and Clark, 1995). Conceptually, Eq. 5 attributes the bubble-size distribution to be the distribution implied by the number of largest chord lengths corresponding to each bubble size, less those chord lengths arising from off-center cuts of bubbles of greater size. However, a probability function $P_c(y)$ has to be found first to fit chord-length data. Oftentimes, the model form of the probability function $P_c(y)$ is not known, and this is the shortcoming of a parametric approach. A new general approach presented below offers an effective alternative.

Parzen window density function estimator

Let $X_1, X_2, \ldots, X_n$ (samples) be independent random variables identically distributed as random variables X, the distribution function of which $F(x) = P[X \le x]$ is absolutely continuous

$$F(x) = \int_{-\infty}^{x} P(z)\, dz, \qquad (6)$$

with probability density function $P(x)$.

As an estimate of the value $F(x)$ of the distribution function at a given point x, it is natural to take the sample distribution,

$$F_n(x) = (1/n)\{\text{no. of observations} \le x \text{ among } X_1, \ldots, X_n\}. \qquad (7)$$

Various possible estimates of the probability density functions suggest themselves, but none of them appears to be naturally superior. For example, as an estimate of $P(x)$ one might take

$$P_n(x) = \frac{F_n(x+h) - F_n(x-h)}{2h}, \qquad (8)$$

where h is a positive number. However, one must address the suitable choice of h.

The window method described by Parzen (1962) is the technique used to estimate the probability density function from a given set of data. Each point in the sample is designated as a unit center, and an identical basis function is constructed at each point. The functional form of the estimator is

$$P_n(x) = \frac{1}{nh} \sum_{i=1}^{n} \Psi\left(\frac{x - X_i}{h}\right), \qquad (9)$$

where n is the sample size, X_i is the sample point, h is the window width, x is a point in the variable distribution space, and $\Psi(u)$ is a Barel function (Johnston and Kramer, 1994) that satisfies the following criteria to ensure $P_n(x)$ is a valid density function:

$$\int_{-\infty}^{\infty} \Psi(u)\, du = 1 \qquad (10)$$

$$|\Psi(u)| < \infty \quad \text{for } -\infty < u < \infty \qquad (11)$$

$$\lim_{u \to \infty} |u\Psi(u)| < \infty \qquad (12)$$

$$\lim_{n \to \infty} h(n) = 0 \qquad (13)$$

$$\lim_{n \to \infty} nh^2(n) = \infty. \qquad (14)$$

Parzen (1962) has proven that the estimated probability density function $P_n(x)$ tends uniformly (in probability) to the true probability density function. In other words, the Parzen window estimator, $P_n(x)$, will converge to the true probability distribution of the data, $P(x)$, in the limit of an infinite data set. Equations 11 and 12 ensure that $\Psi(u)$ is bounded in the vertical and horizontal direction, respectively, and Eqs. 13 and 14 impose conditions on the choice of the window width $h(n)$ as a function of the number of data points, n, to ensure that the window size shrinks to zero, although at a slower rate than the growth of the number of data points. There are many different forms of basis functions, $\Psi(u)$: the one most often used is a spherically symmetrical Gaussian form, which is described as,

$$\Psi(u) = \frac{1}{\sqrt{2\pi}} e^{-u^2/2}. \qquad (15)$$

Ultimately, the estimated probability density function can be represented as

$$P_n(x) = \frac{1}{nh\sqrt{2\pi}} \sum_{i=1}^{n} e^{-1/2((x-X_i)/h)^2}. \tag{16}$$

Estimated density function of local bubble-size distribution

Since a set of chord-length data $[y_1, y_2, \ldots, y_n]$ is available, the Parzen window estimator for the probability density function can be employed to evaluate the probability density distribution function of chord lengths. This function, $P_c(y)$, can be constructed by substituting y for x and y_i for X_i into Eq. 16. Finally, by substituting $P_c(y)$ and its derivative $dP_c(y)/dy$ into Eq. 4, one finds that

$$P_p^e(R) = \frac{\alpha}{nh\sqrt{2\pi}} \sum_{i=1}^{n} e^{-(2\alpha R - y_i)^2/2h^2} + \frac{2\alpha^2 R}{nh^3\sqrt{2\pi}} \sum_{i=1}^{n} (2\alpha R - y_i) e^{-(2\alpha R - y_i)^2/2h^2}, \tag{17}$$

where $R = y/2\alpha$.

The information needed for Eq. 17 is only the available chord-length data, since the bubble shape factor is already known. There is no probability density function required to fit chord lengths, as has previously been used in the analytical backward transform method (Liu and Clark, 1995). This means that the chord-length data may be interpreted into a local bubble-size density distribution directly, when chord-length data and the bubble-shape factor α are known. The estimate of $P_p(R)$ (the local bubble-size distribution) is then constructed by using Eq. 17. This equation is valid only for the ellipsoidally shaped bubble model. For truncated ellipsoidally shaped bubbles used previously to model spherical cap bubbles in fluidized beds, one is obliged to use a "best-fit" ellipsoidal shape, because analysis using the truncated ellipsoid proves too intractable.

Equation 17 is an estimator for the local bubble-size density distribution. The definition of a probability density function requires that it be nonnegative and that it integrate to unity over the entire space. Integrating Eq. 17 with respect to R between the appropriate limits proves that the probability function satisfies the necessary condition (Liu, 1995). However, it is hard to prove that the estimator is nonnegative. The first term in Eq. 17 is always nonnegative for all values of R, but the sign of the second term depends on the sign of $(2\alpha R - y_i)$. Nevertheless, a certain set of chord-length data is always uniquely related to a certain bubble-size distribution. In other words, the chord-length distribution is not arbitrary, and is formed based on the local bubble-size distribution. So nonnegative values of $P_p^e(R)$ could be maintained for a set of reasonable chord-length data. This fact will be demonstrated below in the simulation and discussion section.

Optimal model structure

Before chord-length data are processed, the width h of the Parzen window function has to be chosen with due regard to the size of sample set. When one (as always) has a finite data set, an optimal estimator with a particular value of h will exist. The choice of the Parzen window width should be based on a measure of performance and presumably results should not change violently as h is changed in the neighborhood of its optimal value. Since in practice the researcher is dealing with a set of new, previously unseen data, a reliable approach for h must be identified. The measure of how well a particular estimator approximates a density function (local bubble-size distribution) is defined as the product of the probabilities of sample points independently and randomly drawn from the true underlying distribution (Traven, 1991; Johnston and Kramer, 1994). For a given sample set the overall fit measure is given by

$$J = \prod_{i=1}^{n} P_p^e(R_i), \tag{18}$$

where $R_i = y_i/2\alpha$. For convenience of calculation, usually the log of Eq. 18 is used as a measure of performance,

$$J_{\log} = \log(J) = \sum_{i=1}^{n} \log[P_p^e(R_i)]. \tag{19}$$

The optimal Parzen window width, h, is the value that maximizes the product of the probability for all sample points. This value is also the one most suited to bubble-size density distribution estimation. In other words, when a set of chord-length data is given, the parameter of Parzen window width, h, will be chosen so that $J_{\log}$ has maximum value to obtain the best estimate of the local bubble size density distribution. This will involve performing the transform with several values of h and choosing that result that yields the highest value of $J_{\log}$. Liu (1995) has offered an estimator for the best h as

$$h = \frac{\sqrt{(\text{mean } y)(\text{std. dev. } y)}}{\sqrt[5]{n}},$$

where n is the sample size.

Simulation and Discussion

Monte-Carlo simulation was used to generate bubbles synthetically around an "imaginary" probe to get a set of chord-length data. Although the authors have experimental chord-length data available (Liu, 1995), corresponding bubble-size distributions were not measured directly. Accordingly, a certain number of bubbles were produced based on a specified local bubble-size probability density distribution $P_p(R)$, and chord lengths were calculated by

$$y = 2\alpha\sqrt{R^2 - r^2}. \tag{20}$$

Then, Eq. 17 was employed to find the best estimate of the local bubble-size probability density function $P_p(R)$ with the

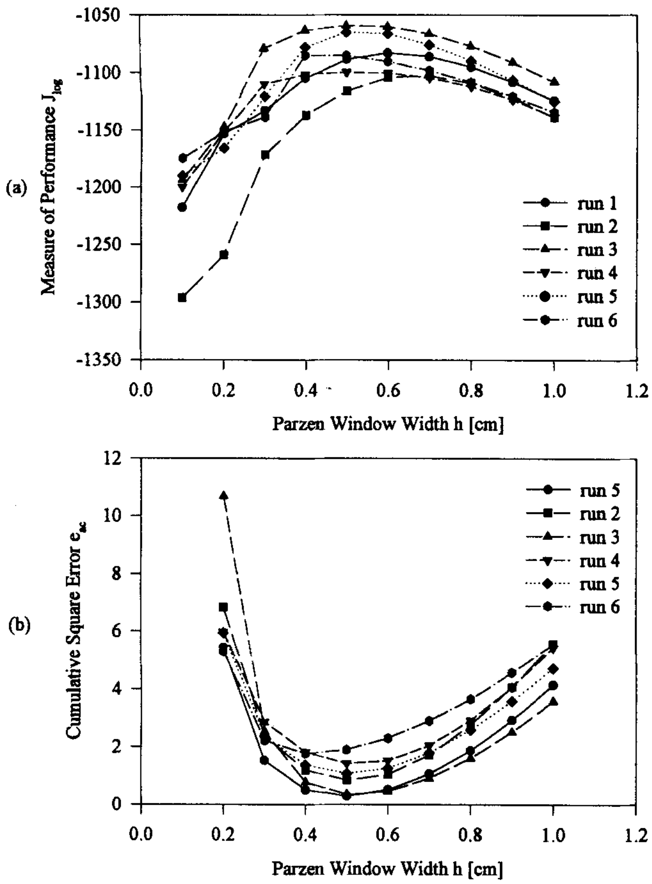

Figure 3. Six hundred sample-size Monte-Carlo simulations.

(a) The measures of performance, and (b) the cumulative square errors of the six runs for different Parzen window width, h.

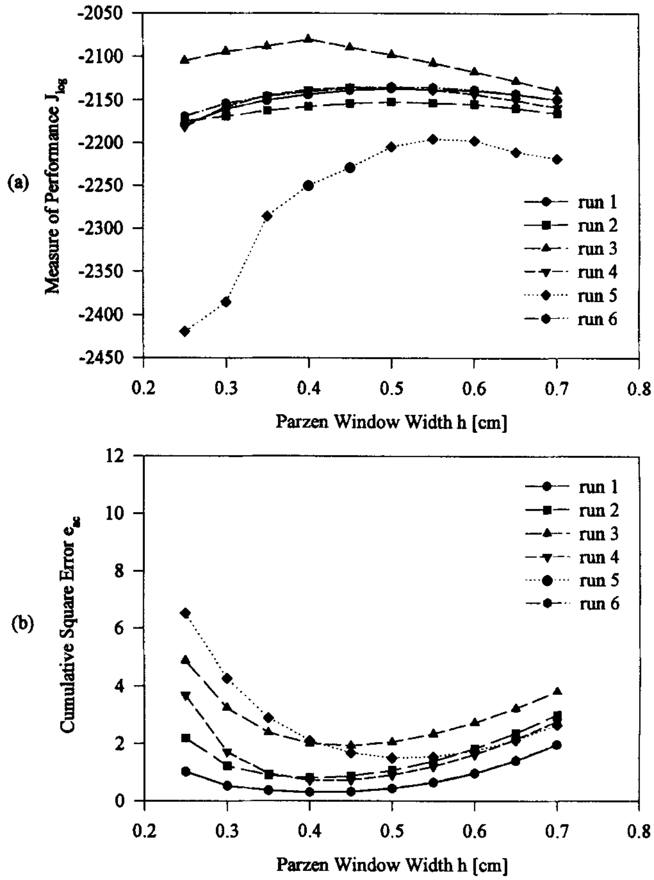

Figure 4. Twelve hundred sample-size Monte-Carlo simulations.

(a) The measures of performance, and (b) the cumulative square errors of the six runs for different Parzen window width, h.

optimal Parzen window width, h, for a set of available chord-length data. This is the procedure for directly transforming chord-length data to the local bubble-size density distribution.

Simulations were conducted based on the example case where

$$P_p(R) = \frac{R^3}{2\mu^4} e^{-R^2/2\mu^2},$$

a modified Rayleigh probability function, where $R \geq 0$ and $\mu = 1.4$, and the bubble-shape factor $\alpha = 0.6$. This function was chosen as an example and is suitable because it has zero probability for $R < 0$. The six runs were conducted for both 600 and 1,200 bubble sample sizes, respectively. The measures of performance $J_{\log}$ and the cumulative square errors between estimate $P_p^e(R_i)$ and the original value of $P_p(R_i)$, which is defined as

$$e_{ac} = \sum_{i=1}^{n} (P_p^e(R_i) - P_p(R_i))^2, \tag{21}$$

for each run were computed and are illustrated in Figures 3 and 4 for 600 and 1,200 bubble sample sizes, respectively. Those figures show that the measure of performance and the cumulative square error vary with Parzen window width for each run, and that the measure of performance increases to a specific value and then decreases, while the cumulative square error decreases to a certain point and then increases as the Parzen window width decreases from a large value. There exists the maximum $J_{\log}$ and the minimum cumulative square error (i.e., the least-square error) for each run. The figures also show that the values of $P_p^e(R)$ are similar whether h is chosen using the measure of performance, $J_{\log}$, or the minimum cumulative square error, e_{ac}. The average values of the measures of performance $J_{\log}$ and the cumulative square errors of the six runs for the two sets of sample size are illustrated in Figures 5 and 6, respectively. Good agreement is evident.

The minimum values of average cumulative square errors are 0.9782 for the 600 bubble sample size and 0.9824 for the 1,200 bubble sample size. So the normalized minimum value of average cumulative square error of the 1,200 bubble sample (0.9824/1,200) is less than that of the 600 bubble sample (0.9782/600). The maximum values of the average measure of performance $J_{\log}$ for the 600 and the 1,200 bubble samples

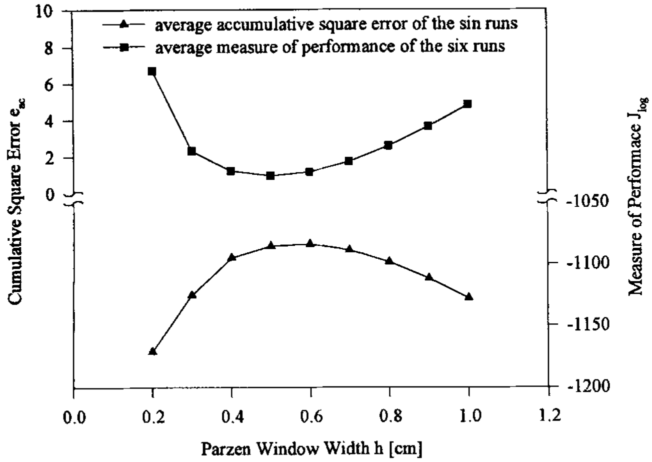

Figure 5. Average values of the measure of performance and cumulative square errors for the six runs with different Parzen window width, *h*, where the bubble sample size is 600.

are −1,083.9 and −2,143.3, respectively. Obviously, the normalized maximum value of average measure of performance $J_{\log}$ of the 1,200 bubble sample size (−2,143.3/1,200) is greater than that of the 600 bubble sample size (−1,083.9/600). These phenomena suggest that the accuracy of the estimate $P_p^e(R)$ increases as the sample size increases, which is to be expected. Figure 7 illustrates that the optimal estimate of $P_p^e(R)$ for the 1,200 bubble sample is closer to its original distribution than that for the 600 bubble sample. For the same set of samples, when h is greater than the optimal values (Parzen window becomes wide), the estimate of $P_p(R)$ becomes flat and the variance of the estimate $P_p^e(R)$ increases, and when h is less than the optimal value (Parzen window becomes narrow), the estimate of $P_p^e(R)$ becomes spiky (there are artifacts in the transform) and the cumulative error increases as shown in Figures 8 and 9. From comparison of Figure 5 with Figure 6, one finds that the optimal value of h

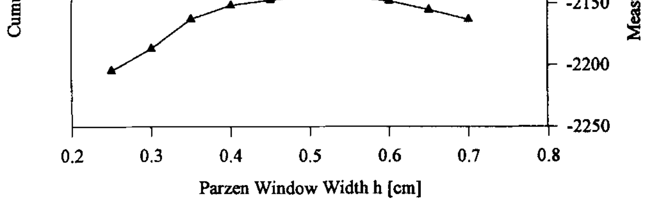

Figure 6. Average values of the measure of performance and cumulative square errors for the six runs with different Parzen window widths with 1,200 bubble sample size.

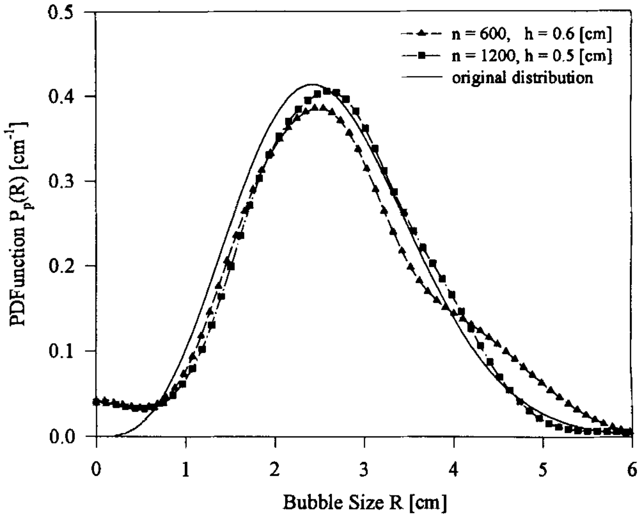

Figure 7. Best estimates of the local bubble-size density distribution for the 600 and 1,200 bubble samples (one of the six runs) and the original distribution.

decreases as the sample size (the number of bubbles touching the probe) increases. These results are in agreement with the requirement of Eq. 13.

One may find there are more errors in the prediction of the local bubble-size density distribution at very small bubble sizes (called local error). There are two reasons contributing to computation errors. One is the basis function for the density function estimator, which is the Gaussian form. All the data within the Parzen window contribute to the value of the estimation function at a specific point that is located within the Parzen window. Reducing the Parzen width, h, can decrease the local errors. However, if the window width is less than the optimal value, the global estimates of the density function are apt to become "spiky" (or unstable) and the

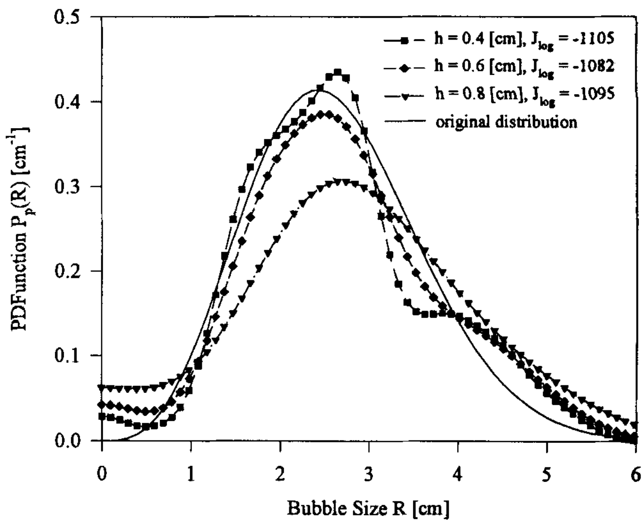

Figure 8. Estimates of the local bubble-size distribution of the 600 bubble samples for different Parzen window width, *h* (one of the six runs), and the original distribution.

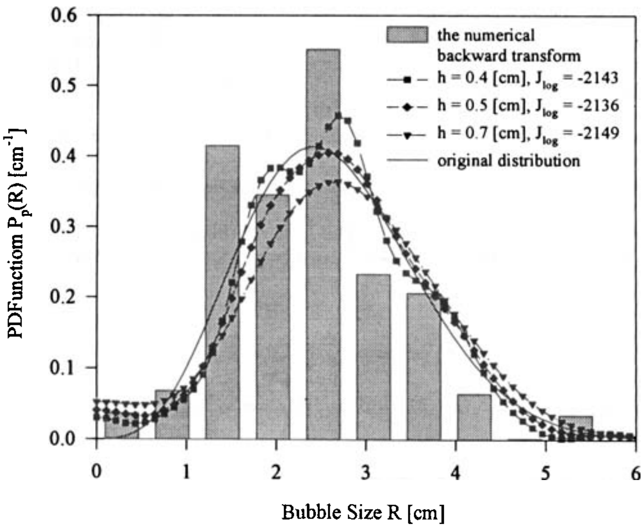

Figure 9. Estimates of the local bubble-size distribution of the 1,200 bubble samples for different Parzen window width, *h* (one of the six runs), the estimate of the local bubble-size distribution found by using the numerical backward transform (10 bins in bubble size), and the original distribution.

global errors increase. The other reason is that the Monte-Carlo simulation is a probabilistic simulation. The chord-length data are therefore generated randomly and cannot be expected to be the same as the theoretical continuous distribution. The choice of the Parzen window width should be based on the optimal structure, as mentioned earlier, so as to obtain the best global estimation.

The maximum measure of performance approach is more feasible and effective than the minimum cumulative square error approach. This is because the minimum cumulative square error approach needs information about the original local size density distribution of bubbles, which is not known, to evaluate the cumulative square error between the estimate $P_p^e(R)$ and the original values. However, the information needed to compute the measure of performance $J_{\log}$ is all the information needed to compute the estimate of local bubble-size density distribution $P_p(R)$, that is, the measured chord-length data and bubble-shape factor. Moreover, the results gained using the maximum measure of performance approach have a good agreement with ones of the minimum cumulative square errors approach.

The new approach has been compared with the numerical backward transform method presented by Clark and Turton (1988), and conditions have been chosen to introduce instability in the numerical transform. The same set of chord-length data as in Figure 9 was processed by the numerical backward transform method with 10 subdivisions in the bubble-size range (the size interval $\Delta R = 0.52$ for each), and the results are illustrated with 10 bars in the same figure. Figure 9 shows that the results from numerical backward transform are far from the original values due to instability. However, the results from the window approach show superior agreement. This suggests that the new approach offered in this article is a more accurate and stable approach for inferring local bubble-size distribution from chord-length data directly and has a stronger ability to tolerate errors in the original data.

Conclusions

A new general approach using a Parzen window estimator has been proposed for interpreting chord-length data directly to the local bubble-size distribution without requiring information about the nature of chord-length distribution. The Parzen window width, h, is determined by the measure of performance, $J_{\log}$, and the optimal value of h is the one that maximizes the measure of performance. Monte-Carlo simulations demonstrate that the local bubble-size density distribution estimated by using the nonparametric approach from the chord lengths simulated has a good agreement with the theoretical distribution, and that the approach can provide better prediction as the number of samples increases.

Acknowledgment

The authors are grateful for support of this research to the National Science Foundation, grant CTS-8957146.

Notation

Ψ = Parzen window function
μ = parameter of modified Rayleigh probability function (cm)

Subscripts and superscripts

c = chord length
p = bubbles intersecting the probe
e = estimated function

Literature Cited

Atkinson, C. M., and N. N. Clark, "Analysis of Fluidized Bed Behavior Using Probes," *Proc. Power Bulk Solid Conf.*, Rosemont, IL, p. 437 (1986).

Burgess, J. M., A. G. Fane, and C. J. D. Fell, "Application of an Electroresistivity Probe Technique to a Two-Dimensional Fluidized Bed," *Trans. Instn. Chem. Engrs.*, **60**, 249 (1981).

Cheremisinoff, N. P., "Review of Experimental Methods for Studying the Hydrodynamics of Gas-Solid Fluidized Beds," *Ind. Eng. Chem. Process Des. Dev.*, **25**, 329 (1986).

Chiba, T., K. Terashima, and H. Kobayashi, "Lateral Distribution of Bubble Sizes in Two-Dimensional Gas-Fluidized Bed," *J. Chem. Eng. Japan*, **8**, 167 (1975).

Clark, N. N., and R. Turton, "Chord Length Distributions Related to Bubble Size Distributions in Multiphase Flows," *Int. J. Multiphase Flow*, **14**, 413 (1988).

Clark, N. N., E. A. McKenzie, and M. Gautam, "Differential Pressure Measurements in a Slugging Fluidized Bed," *Powder Technol.*, **67**, 187 (1991).

Clark, N. N., R. Seiss, and R. Turton, "Probe Measurement in Gas-Liquid System," *Flow Meas. Instrum.*, **3**, 9 (1992).

Ishida, M., T. Shirai, and A. Nishiwaki, "Measurement of the Velocity and Direction of Flow of Solid Particles in a Fluidized Bed," *Powder Technol.*, **27**, 1 (1980).

Johnston, L. P., and M. A. Kramer, "Probability Density Estimation using Elliptical Basis Functions," *AIChE J.*, **40**, 1639 (1994).

Judd, M. R., and P. Dixon, "The Flow of Fine, Dense Solids down a Vertical Standpipe," *AIChE Symp. Ser.*, **74**(176), 38 (1978).

Lee, S., A. Soria, and H. Lasa, "Evolution of Bubble Length Distributions in Three-Phase Fluidized Beds," *AIChE J.*, **36**, 1763 (1990).

Lim, K. S., and P. K. Agarwal, "Conversion of Pierced Lengths Measured at a Probe to Bubble Size Measures: An Assessment of the Geometrical Probability Approach and Bubble Shape Models," *Powder Technol.*, **63**, 205 (1990).

Liu, W., PhD Diss., West Virginia Univ., Morgantown (1995).

Liu, W., and N. N. Clark, "Relationships between Distribution of

Chord Lengths and Distributions of Bubble Sizes Including their Statistical Parameters," *Int. J. Multiphase Flow*, **21**, 1073 (1995).
Matsen, J. M., "Evidence of Maximum Stable Bubble Size in a Fluidized Bed," *AIChE Symp. Ser.*, **69**(128), 31 (1973).
Oki, K., T. Akehata, and T. Shirai, "A New Method for Evaluating the Size of Moving Particles with a Fiber Optic Probe," *Power Technol.*, **11**, 51 (1975).
Oki, K., W. Walawender, and L. T. Fan, "The Measurement of the Local Velocity of Solid Particles," *Power Technol.*, **18**, 171 (1977).
Parzen, E., "On Estimation of a Probability Density Function and Mode," *Ann. Math. Stat.*, **33**, 1065 (1962).
Rowe, P., and R. Matsuno, "Single Bubbles Injected into a Gas Fluidized Bed and Observed by X-Rays," *Chem. Eng. Sci.*, **26**, 923 (1971).
Sitnai, O., "Utilization of the Pressure Differential Records from Gas Fluidized Beds with Internals for Bubble Parameters Determination," *Chem. Eng. Sci.*, **37**, 1059 (1982).
Traven, H. G., "A Neural Network Approach to Statistical Pattern Classification by 'Semiparametric' Estimation of Probability Density Functions," *IEEE Trans. Neural Networks*, **NN-2**, 366 (1991).
Turton, R., and N. N. Clark, "Interpreting Probe Signals from Fluidized Beds," *Powder Technol.*, **59**, 117 (1989).
Werther, J., "Bubbles in Gas Fluidized Beds: I," *Trans. Instn. Chem. Engrs.*, **52**, 149 (1974a).
Werther, J., "Bubbles in Gas Fluidized Beds: II," *Trans. Instn. Chem. Engrs.*, **52**, 160 (1974b).
Werther, J., and O. Molerus, "The Local Structure of Gas Fluidized Beds: I. A Statistically Based Measuring System," *Int. J. Multiphase Flow*, **1**, 101 (1973).

Manuscript received Aug. 30, 1995, and revision received Mar. 7, 1996.